Room-temperature phonon boundary scattering below the Casimir limit

Jyothi Sadhu and Sanjiv Sinha

Phys. Rev. B **84**, 115450 — Published 26 September 2011

DOI: 10.1103/PhysRevB.84.115450

Room Temperature Phonon Boundary Scattering Below the Casimir Limit

Jyothi Sadhu and Sanjiv Sinha*

Department of Mechanical Science and Engineering,

University of Illinois, Urbana, Illinois 61801

Abstract

Thermal conductivity data for rough surface silicon nanowires suggest the breakdown of the Casimir limit which assumes completely diffuse phonon boundary scattering. We show that coherent effects in phonon transport at room temperature indeed lead to such breakdown. Correlated multiple scattering of phonons off the rough surface lead to a reduced thermal conductivity that is dependent not just on the roughness amplitude but more importantly on the roughness correlation length. A correlation length less than diameter of wire is typically necessary for lowering the thermal conductivity below the Casimir limit. Our model explains seeming anomalies in data reported for electrolessly etched and electron beam lithography defined nanowires.

I. INTRODUCTION

Recent measurements of the thermal conductivity of electrolessly etched silicon nanowires[1,2] claim a thermal conductivity as low as $\sim$ 3 W/mK at room temperature for a 50 nm diameter wire. This intriguing fifty-folds reduction from the value for the bulk is well below the Casimir limit[3] and close to the amorphous limit of $\sim$1 W/mK for silicon. What is even more puzzling is that measurements on wires fabricated using electron-beam lithography and roughened using reactive-ion etching [2] do not exhibit the anomalously low thermal conductivities as the electrolessly etched wires even though their surface roughness exceeds that of the electrolessly etched wires. While further measurements are still needed to verify these results, these initial experiments draw attention to a deeper examination of the validity of the Casimir limit in nanostructures. The Casimir limit[3] of phonon boundary scattering, based on complete thermalization of incident phonons at the boundaries of a crystal, yields a phonon mean free path comparable with the crystal dimensions. For a wire geometry, the theory yields a phonon mean free path equal to the wire diameter. A 50 nm diameter single-crystal silicon wire is expected to have a thermal conductivity of $\sim$20 W/mK at room temperature at the Casimir limit of boundary scattering, much higher than that reported for electrolessly etched wires.

Existing theoretical work[4–8] explain the reduction in thermal conductivity using different approaches. Atomistic simulations[4] show that the low thermal conductivity arises due to non-propagating vibrational modes. The computations are restricted to diameters of 4 nm and do not facilitate a direct comparison with experimental data. Monte Carlo modeling of phonon transport[5] using frequency dependent surface scattering matches reasonably with data but predicts a continuously decreasing thermal conductivity with increasing roughness amplitude and contradicts the measurements on the electron-beam defined wires[2]. A subtle issue in the formulation is the use of a scattering cross-section[9] that is valid for bulk disorder. The wires, especially at a low doping, do not appear to possess any bulk disorder according to the available TEM evidence. The model also counts surface scattering twice by including the frequency independent Casimir limit along with the frequency dependent scattering. Thus, it is difficult to ascertain if the fit to experimental data is fortuitous rather than physical.

A third model[6–8] approaches the problem through an examination of coherent effects.

This applies Morse's results[10] for a disordered linear chain to obtain a mean free path for surface scattering and uses it along the lines of the DMPK theory[13]. The results explain low temperature data satisfactorily but do not address the room temperature behavior. In this paper, we build on such coherent transport theory[6,8] to consider roughness dependent multiple scattering in conjunction with Umklapp scattering. The consideration of Umklapp scattering is necessary for predicting room temperature behavior but introduces the complexity of treating coherent and incoherent scattering simultaneously. Our model handles this by separating transport into distinct frequency dependent regimes where coherent or incoherent scattering dominate. We find that the multiple scattering of phonons from correlated points on the wire surface lead to strong attenuation. The mean free path from multiple scattering is shorter than that from Umklapp scattering across a range of frequencies, even at room temperature. Such scattering leads to conductivity well below the Casimir limit for high frequency phonons. However, it is not just the roughness amplitude but also the roughness correlation that decides the overall conductivity.

II. GENERAL FORMALISM

A. Model

In order to consider coherent phonons, we start with a wave treatment of phonon transport. The interaction of phonons with the randomly rough walls of the nanowire leads to an attenuation of the mean intensity. To estimate the mode dependent attenuation, we derive the phase shift induced by the surface roughness. We consider a wire of length L along the x-direction. Rough walls are present along the y- and z-directions such that $0 \leq y \leq a$; $0 \leq z \leq b$ define the wire dimensions. We note that experimental nanowires are typically not cylindrical. When comparing with diameter dependent experimental data, we define the characteristic diameter, $d = \sqrt{4ab/\pi}$. We use individual scalar wave equations to describe polarizations of phonons in the wire, implicitly ignoring coupling between polarizations enabled by the disorder. By comparison with experimental data later, we show that this simplifying assumption is still adequate in illustrating the basic physics.

To obtain the phase shift, we need the Green function, G, for phonons in the rough wire.

This modified Green function can be obtained from the Green function of a smooth wire G_0 as described below. The Green function G_0 for a smooth square wire is a solution of Helmoltz equation with a stress free boundary condition over its smooth walls $\mathbf{S}$ given as

$$\left(\nabla^2 + K^2\right)G_0(R, R_0) = -4\pi\delta(R - R_0) \tag{1}$$

$$\partial G_0/\partial n|_{\mathbf{S}} = 0 \ , \tag{2}$$

where the outward normal to $\mathbf{S}$ is $\overrightarrow{n}$, K is the total wave number, R and R_0 are the point of observation and the source respectively.

In defining the boundary condition, we hypothesize that the surface responsible for scattering phonons is the interface between the crystal and the surface oxide and not the outer surface. Our hypothesis follows from existing transmission electron micrographs of the rough nanowires [1]. While an impedance boundary condition is more appropriate here, the transmission coefficient of phonons between silicon and its native oxide remains unknown theoretically and experimentally. Thus, we choose to use a stress free condition for mathematical convenience. We have performed computations with frozen boundary condition ($G_0 = 0$ at surface $\mathbf{S}$) and do not find a significant impact of the choice of boundary condition. We note that the oxide thickness is ~ 2 nm and we do not expect the thin oxide itself to play a dominant role in surface scattering.

The solution for Eq (2) for a three dimensional waveguide $\mathbf{R} = \{x, y, z\}$ can be expressed as[8]

$$G_0(R, R_0) = \int_{-\infty}^{\infty} \frac{d\kappa}{2\pi} e^{i\kappa(x-x_0)} \sum_m \sum_n \frac{\phi_{mn}(y, z)\phi_{mn}(y_0, z_0)}{k^2 + (n\pi/a)^2 + (m\pi/b)^2 - K^2} \tag{3}$$

where a and b are cross sectional dimensions of the square wire and the transverse eigenfunctions $\phi_{mn}(R)$ are given by

$$\phi_{mn}(x, y, z) = \frac{2\epsilon_{mn}}{(ab)^{1/2}} \ cos\left(\frac{n\pi y}{a}\right) cos\left(\frac{m\pi z}{b}\right) exp(i\kappa_{mn}x) \tag{4}$$

where $\kappa_{mn}^2 = K^2 - (n\pi/a)^2 - (m\pi/b)^2$ is the longitudinal wavevector; $\epsilon = 1/2$ for $m = n = 0$ and is unity otherwise.

To obtain the modified Green function in the same volume with random perturbation in the surface profile $\mathbf{S}$, we solve Eq. (1) with the boundary condition in Eq. (2) applied over the

random rough surface $\Re$ instead of $\mathbf{S}$. If the rough boundary at the bottom of the square nanowire is assumed $z = \zeta(x)$ where $\zeta(x)$ represents the random surface height along the wire length, we can enforce the stress free condition as $\partial G/\partial n|_{\Re} = 0$. We then project the boundary conditions on the rough surface, $\Re$ onto the smooth boundaries $\mathbf{S}$ by expressing the surface normal on $\Re$ as $\overrightarrow{n} = -\overrightarrow{z} + \zeta'(x)\overrightarrow{x}$ where $\zeta'(x) = d\zeta/dx$ is the random slope of $\Re$. Hence the boundary condition for the rough wire becomes

$$\frac{\partial G}{\partial n}\Big|_{\Re} = \left(-\frac{\partial G}{\partial z} + \zeta'(x)\frac{\partial G}{\partial x}\right)\Big|_{z=\zeta(x)} = 0. \tag{5}$$

Expanding Eq. (5) about the smooth boundary $z = 0$ in terms of ζ and ζ', retaining only first order derivates, we obtain

$$\left(\frac{\partial G}{\partial z} + \zeta\frac{\partial^2 G}{\partial z^2} - \zeta'\frac{\partial G}{\partial x}\right)_{z=0} = 0 \tag{6}$$

By using Green theorem, we can express the Green function in rough wires as

$$G(R, R_0) = G_0(R, R_0) + \frac{1}{4\pi}\int_S \left(G(R, r)\frac{\partial G_0(r, R_0)}{\partial n} - G_0(R, r)\frac{\partial G(r, R_0)}{\partial n}\right)\, dr \tag{7}$$

where $r \in \mathbf{S}$. Substituting the boundary conditions in Eq. (6) and Eq (2) into Eq. (7), we obtain

$$G(R, R_0) = G_0(R, R_0) + \frac{1}{4\pi}\int_S G_0(R, r)\widehat{V}(r)G(r, R_0)\, dr \tag{8}$$

where the operator $\widehat{V}(r)$ with $r \equiv \{x, y, z\}$ is given by

$$\widehat{V}(r) = \zeta\frac{\partial^2}{\partial z^2} - \zeta'\frac{\partial}{\partial x} \tag{9}$$

Applying an iteration method, we substitute the Green function $G(r, R_0)$ on left hand side of Eq. (8) with the Green function from i^{th} iteration $G^{(i)}(R, R_0)$ thus obtaining an infinite series expansion for $G(R, R_0)$ as shown in Eq. (10)

$$\begin{aligned} G(R, R_0) = G_0(R, R_0) &+ \frac{1}{4\pi}\int G_0(R, r)\widehat{V}(r)G_0(r, R_0) \\ &+ \frac{1}{(4\pi)^2}\int\int G_0(R, r_1)\widehat{V}(r_1)G_0(r_1, r_2)\widehat{V}(r_2)G(r_2, R_0)\, dr_1 dr_2 + \dots \end{aligned} \tag{10}$$

Thus the n^{th} term in this series is a n-fold integral over the surface involving n functions $\widehat{V}(r_i)$ $(i = 1, 2, 3 \dots n)$ and represents the n^{th} order scattering field at a point R from the roughness aspersions due to source at R_0.

The first statistical moment $\langle G(R,R_0)\rangle$ represents the field intensity at point R coherent with the source at R_0. Hence the spatial decay of averaged Green function yields the length over which coherence is lost due to the boundary scattering. We proceed with ensemble averaging of the Green function from Eq. (8) over statistical realizations of ζ. To this purpose, we assume the random function ζ is statistically uniform and varies only along the wire length (x), we assign normal Gaussian statistics to ζ such that $\langle\zeta(x)\rangle$=0, $\langle\zeta^2(x)\rangle$=0 and the spatial correlation function is

$$\langle\zeta(x_1)\zeta(x_2)\rangle = \sigma^2 exp(-|x_1-x_2|^2/L_c^2) \tag{11}$$

Here σ is root mean square height of surface ζ and L_c is its correlation length. Thus averaging Eq. (10) and noting that all the odd-moments of the random operator $\widehat{V}(r)$ vanish, we finally obtain

$$\langle G(R,R_0)\rangle = G_0(R,R_0) + \frac{1}{(4\pi)^2}\int\int_S G_0(R,r_1)\widehat{M}(r_1,r_2)\langle G(r_2,R_0)\rangle\ dr_1 dr_2 \tag{12}$$

where the mass operator $\widehat{M}(r_1,r_2)$ is the sum of infinite terms representing increasing order of correlations in $\widehat{V}$. The first term of the mass operator is $\langle\widehat{V}(r_1)G_0(r_1,r_2)\widehat{V}(r_2)\rangle$ and we retain only this term which is the so-called Born approximation in volume scattering theory[12]. The solution of Eq. (12) which resembles Dyson equation can be solved using spatial Fourier transform outlined in Ref. 11.

Finally we expand the averaged Green function in plane waves $exp[i\overline{\kappa}_r r]$ where $\overline{\kappa}_r$ is the perturbed wavenumber due to roughness. The unperturbed wavenumber κ_{mn} (Eq. (4)) thus shifts by $\delta\kappa_{mn}$=$\overline{\kappa}_{mn}-\kappa_{mn}$. This shift is proportional to the mass operator and the derivative of the unperturbed eigenfunctions ϕ_{mn} in Eq. (4) with respect to the Fourier variable κ. The mean attenuation length of wave intensity is obtained from the imaginary part of this wavenumber shift $\mathrm{Im}(\delta\kappa_{mn})$ as $l = [2\mathrm{Im}(\delta\kappa_{mn})]^{-1}$ .For phonon mode with transverse wavenumbers $\{m,n\}$, we obtain the mean attennuation length as

$$l_{mn}(\omega)^{-1} = \left(\frac{\sigma}{d}\right)^2 \frac{2\epsilon_{mn}}{\kappa_{mn}} \sum_p \sum_q \sum_{\alpha=0,\pi} \frac{\epsilon_{pq}(K^2-\kappa_{mn}\kappa_{pq}\cos\alpha)^2}{\kappa_{pq}} \widetilde{W}(|\kappa_{mn}-\kappa_{pq}|), \tag{13}$$

where m, n, p and q are indices representing phonon modes, κ is the longitudinal wave number, α is the angle between incident (mn) and scattered directions (pq). The Fourier

transform of the wall roughness correlation function is given by $\widetilde{W} = \sqrt{\pi} L_c exp(-\kappa^2 L_c^2/4)$; $K = \omega/c$ is the wave number of the phonon propagating at speed c. The summation in Eq. 13 represents the sum of scattering probabilities of the incident field mn into all possible incoherent channels where the probability for scattering into a particular channel pq is proportional to the correlation function $\widetilde{W}(\kappa_{mn} - \kappa_{pq})$. The double summation runs over all modes p, q that satisfy $\sqrt{p^2 + q^2} < \omega d/c$ representing the total phonon modes $N(\omega)$ at the frequency ω.

B. Phonon transmission coefficient

We proceed with calculating the attenuation length of every eigenmode ϕ_{mn} of a square wire using Eq. (13) with appropriate choice of roughness parameters σ and L_c. Figure 1(a) plots the logarithm of inverse of the mean field attenuation length ($log_{10}\ l_{mn}$) as a function of phonon frequency and wave number. Three distinct transport regimes become evident: Quasi-ballistic, weakly localized and diffusive. We now discuss each of the regimes individually. The quasi-ballistic regime is restricted to the fundamental modes ($\omega \sim k$) with long wavelengths. These modes see the surface corrugations as point-like imperfections and propagate quasi-ballistically until scattered by Umklapp processes. Since the attenuation length exceeds the length of wire, the transmission function is given by $t(\omega) = 1 - L/l$. In contrast, high frequency and long wavelength modes with large transverse wave vectors, $k_\perp$ are strongly attenuated. Using the results of the DMPK theory[13], the phonon localization length is Nl, where N is the number of phonon modes at frequency ω. When $Nl << L$, the transmission of these phonon modes $t(\omega) = \exp(-L/Nl)$. Even though the model predicts these to be localized, it is likely that these can still propagate particle-like between scatterers[6,14]. In any case, their contribution to thermal conductivity is small due to their low group velocities. Overall, we do not expect a detectable localization behavior in thermal conductivity. We confirm this assertion later with calculations.

All other modes are diffusive and fall into the third and most dominant regime. The transmission function is $t(\omega) = l/L$, where the frequency dependence of l yields the overall frequency dependence of surface scattering. In the Casimir limit, this becomes frequency

independent and l is replaced by the diameter of the wire. We note that the above arguments apply only when the attenuation length, l is smaller than the Umklapp scattering mean free path, Λ_u at the same frequency. In the absence of this condition, surface scattering remains uncorrelated. The effective transmission at the frequency ω, is an average over the transmission coefficient of individual modes $N(\omega)$ in each regime such that $\overline{T_b}(\omega) = \sum_{m,n} t_{mn}/N(\omega)$ where the subscript b represents boundary scattering.

Figure 1(b) compares the mode averaged transmission function $\overline{T_b}(\omega)$ for the Casimir limit with that for multiple scattering. We choose a 50 nm diameter wire and vary the surface roughness to make this comparison. The strong frequency dependence of the low frequency modes is consequential only at very low temperatures. At room temperature, the dominant frequency range is ∼1-7 THz. In smooth wires, the transmission function has contributions above and below the Casimir limit which effectively balances out the frequency dependence. However, as surface roughness increases, the function increasingly deviates below the Casimir limit for high frequency phonons. The sharp discontinuities in the transmission are consequences of mode averaging. The discontinuity in $N(\omega)$ at ~ 5 THz and $\sim 9-10$ is due to the sharp decline of transverse and longitudinal modes respectively at these frequencies which shows up as apparent jump in $\overline{T_b}(\omega)$ in Figure 1(b). We also plot the transmission function for Umklapp scattering for comparison. The delay in the onset of Umklapp scattering is evident in rougher nanowires.

III. THERMAL CONDUCTANCE IN ROUGH WIRES

We use the transmission function to calculate the thermal conductivity of a rough surface nanowire. Following Mingo's approach[15,16], we write the Landauer formula for the thermal conductance of the nanowire,

$$G_{TH} = \sum_{i=1}^{3} \frac{1}{2\pi} \int_0^{\omega_c^i} N_i(\omega) \overline{T_i(\omega)} \hbar\omega \frac{d\langle n\rangle}{dT}\, d\omega \tag{14}$$

where $\langle n\rangle$ is the Bose-Einstein distribution and i represents the polarization of a phonon mode. The cut-off frequency, ω_c for longitudinal modes ($i = 1$), ω_c^L and transverse modes ($i = 2, 3$), ω_c^T are 10 THz and 3.6 THz in accordance with the bulk Si dispersion[17]. The

speed of longitudinal and transverse modes are c_L = 8400 m/s and c_T = 5400 m/s respectively. As temperature increases, the transmission function should include increasing contributions from Umklapp and isotope scattering. The mean free path for isotope scattering, Λ_m=$\langle c \rangle / A\omega^4$ and that for Umklapp scattering, Λ_u=$\langle c \rangle / BT\omega^2 e^{-C/T}$ where $\langle c \rangle$=6400 m/s are added to the transmission function using the Matthiessen's rule. We use values fit to bulk silicon data[15,17]: $A = 1.32 \times 10^{-45} s^3$, $B = 1.7 \times 10^{-19}$ s/K and C = 140 K. The overall transmission function is $\overline{T_i}(\omega) = \left(\overline{T_{b,i}}^{-1} + L/\Lambda_m + L/\Lambda_u \right)^{-1}$.

A. Effect of roughness scales

The two roughness parameters, the root mean square height, σ and the correlation length, L_c affect transport differently. Under the Born approximation, the ratio (σ/d) has an inverse quadratic relation with the attenuation length. Since the transmission function, $\overline{T_b(\omega)}$ is linear in the attenuation length in the dominant diffusive transport regime, the thermal conductance becomes proportional to the inverse of $(\sigma/d)^2$. Figure 2(a) plots the change in room temperature thermal conductivity of a 50 nm silicon nanowire of 2 μm length as the roughness height varies from atomically smooth ($\sim$A^o) to 5 nm. The thermal conductivity dips sharply till σ = 2 nm as the propagation of high frequency phonon modes near the zone center becomes affected. These modes with $\sigma k_\perp >> 1$ are strongly attenuated, consistent with the Rayleigh criterion for destructive interference of the scattered wavefronts. The calculations show that the effect of the roughness height reaches a plateau above σ=4 nm similar to the trend reported in Ref[5]. The present calculations likely overestimate the thermal conductivity at larger values ($\approx$5nm) of σ where terms of order σ^4 would likely increase the attenuation coefficient. However, the trend in roughness height is strongly dependent on the correlation length L_c with an increased sensitivity of the thermal conductivity to roughness height at lower correlation lengths.

The other parameter, the correlation length L_c, affects transport in three ways. First, the inverse of the correlation length controls the Gaussian width of the roughness Fourier spectrum. Strong surface scattering requires the change in phonon wave number on scattering to lie within the Gaussian width. Thus, a short correlation length increases the phase

space for effective multiple scattering, allowing more phonons to participate in the process. A large correlation length reduces the roughness spectrum to a delta-like function. Such roughness can only scatter very long wavelengths, which do not contribute significantly to thermal transport. Second, the correlation length determines the angular spread of intensity in the scattered field, given by $\Delta\Phi \propto (\omega L_c/c)^{-1}$. If a phonon is incident at an angle θ_n from the tangent to the scattering surface, the scattered field in a direction θ_m is proportional to $\exp(-|\cos\theta_n - \cos\theta_m|^2 L_c^2)$. Third, the correlation in relation to the wire diameter controls the cut-off angle for phonons participating in correlated scattering. Phonons incident at angles smaller than $\cot^{-1}(L_c/2d)$ from the surface can not undergo multiple scattering. Figure 2(b) shows the effect of the correlation length on the room temperature thermal conductivity. Quantitatively, the effect of surface roughness on thermal conductivity diminishes when $L_c > 100$ nm.

B. Comparison with data

We now compare the thermal conductivity calculated from the above model with experimental data on electrolessly etched (EE) rough nanowires, electron beam lithography (EBL) defined rough nanowires and vapor-liquid-solid (VLS) grown smooth nanowires respectively. Figure 3 compares the predictions with data for EE wires and Figure 4 shows the thermal conductivity temperature trend for EBL wires across different diameters. We find an excellent agreement with the EE wire data from Ref 1 using the roughness scales, $\sigma = 2.2$ nm and $L_c/d = 0.5 - -0.7$, close to the values reported for these wires from high resolution transmission electron images. We find similar agreement with the data for EBL wires. The thermal conductivity of EBL wires increases approximately four times when compared to EE wires despite an increased roughness height compared to EE wires. This increase results from the large increase in the roughness correlation length in EBL wires compared to EE wires. A nominal rms height, σ =7.4 nm and a correlation length, L_c =400 nm provide a good fit for EBL wires of different cross sections but similar characteristic diameter. Our model also captures the delay in the onset of Umklapp scattering related dip in the thermal conductivity between Wire-1 (120×41 μm^2) and Wire-2 (86×62 μm^2). The reason is the higher boundary scattering rate in the former. As a check, we calculated the thermal

conductivity of smooth VLS grown nanowires assuming small roughness scales. The calculations fit the data for VLS wires ($d > 37$ nm) from Ref 18 using σ =0.4 nm and L_c fixed at 100 nm. The thermal conductivity data for thinned nanowires[7] which show a linear trend in thermal conductivity till 200 K are fit using $\sigma = 1.2$ nm.

In summary, the model described above matches data from all three sets of measurements: VLS smooth wires, EBL rough wires and EE rough wires. The parameters used in fitting, the roughness height and correlation length compare well with experimentally determined values. Despite the reasonable match, we would like to point out a few deficiencies that we seek to address in future work as well as their implications. A major drawback is the use of the Born approximation. The Born approximation essentially replaces the scattered field inside the scattering integral with the incident field. This is valid as long as the scattering is weak, which is expected at small roughness heights and long correlation lengths. While it is difficult to exactly define weak and strong scattering in the present context, we do anticipate that roughened EE wires may correspond to the strong scattering rather than the weak scattering case. Thus, future work should carefully consider higher order scattering terms while still focusing on wires of $\sim$50 nm diameter. Another subtle issue is that the scattering cross-section depends on the second moment of the Green function and not the first statistical moment that we have used in this work. Finally, the roughness statistics in actual wires is likely to be non-Gaussian and may follow a power law. This requires further experimental data but should be relatively easy to consider once such data becomes available.

IV. CONCLUSION

In conclusion, the above quantitative comparisons with existing data lend credence to the existence of coherent effects in phonon surface scattering close to room temperature. We find non-propagating diffusive phonon modes to be the prime conductors of heat in surface disordered nanowires, consistent with molecular dynamics calculations[4] on atomistic scale nanowires. There is no indication of localization in our calculations at the roughness scales reported thus far. We do not observe any length dependence in thermal conductivity, consistent with experimental reports[2]. We note that the model is not without assumptions and the above discussion elaborates on how the assumptions may affect results. However,

removing the assumptions remains challenging at present and will be a focus of future work. Within the assumptions, our model provides insight into the success and failure of the Casimir model. The Casimir model assumes the surface to act as a blackbody phonon emitter and absorber. For a sufficiently smooth surface, the relatively weak frequency dependence in surface scattering leads to the same conductivity as the Casimir limit. Here, "sufficiently" smooth must be carefully defined not just in terms of the roughness height alone, but in terms of the ratio of the roughness height to the characteristic dimension as well as the correlation length. Unlike bulk crystals, the boundary in a nanostructure cannot be considered a blackbody phonon emitter in general. The Casimir limit in this case, should be viewed as a special case rather than the typical behavior.

V. ACKNOWLEDGMENT

Support for this work is in part from ARPA-E under contract DOE-DE-AR-0000041PF-ARRA and in part from the National Science Foundation under the Grant NSF-CBET-09-54696-CAREER. S.S. thanks Bair Budhaev at the University of California, Berkeley for insightful discussions.

---

* sanjiv@illinois.edu

[1] A. I. Hochbaum, R. Chen, R. D. Delgado, W. Liang, E. C. Garnett, M. Najarian, A. Majumdar, and P. Yang, Nature **451**, 163-167 (2008).

[2] K. Hippalgaonkar, B. Huang, R. Chen, K. Sawyer, P. Ercius, and A. Majumdar, Nano Lett. **10**, 4341-4348 (2010).

[3] H. B. G. Casimir, Physica,**5**, 495 (1938).

[4] D. Donadio, and G. Galli, Phys. Rev. Lett **102**, 195901 (2009).

[5] P. Martin, Z. Aksamija, E. Pop, and U. Ravaioli, Phys. Rev. Lett **102**, 125503 (2009).

[6] P. G. Murphy and J. E. Moore, Phys. Rev B **76**, 155313 (2007).

[7] R. Chen, A I. Hochbaum, P. Murphy, J. Moore, P. Yang, and A. Majumdar, Phys. Rev. Lett. **101**, 105501 (2008).

[8] D. H. Santamore and M. C. Cross, Phys. Rev. Lett **87**, 115502 (2001) and Phys. Rev B, **63**, 184306 (2001).

[9] P. Klemens, Solid State Phys. **7**, 1 (1958).

[10] P. M. Morse and K. U. Ingard, *Theoretical Acoustics* (Princeton University Press, Princeton, 1968).

[11] F. G. Bass, V. D. Freulicher, and I. M. Fuks, IEEE Trans. Antennas Propag. **AP-22**, 278-288 (1974).

[12] R.P. Feynman and A.R. Hibbs, *Quantum Mechanics and Path Integrals* (Dover Publications Inc., NY, 1965).

[13] P. A. Mello, P. Pereyra, and N. Kumar, Ann. Phys. (N.Y.) **181**, 290 (1988).

[14] T. R. Kirkpatrick, Phys. Rev. B **31**, 5746-5755 (1985).

[15] N. Mingo, Phys. Rev. B **68**, 113308 (2003).

[16] I. Savic, N. Mingo, and D. A. Stewart, Phys. Rev. Lett. **101**, 165502 (2008).

[17] M. G. Holland , Phys. Rev. 132, 2461-2471 (1963).

[18] D. Li, Y. Wu, P. Kim, L. Shi, P. Yang, and A. Majumdar, Appl. Phys. Lett. **83**, 2934 (2003).

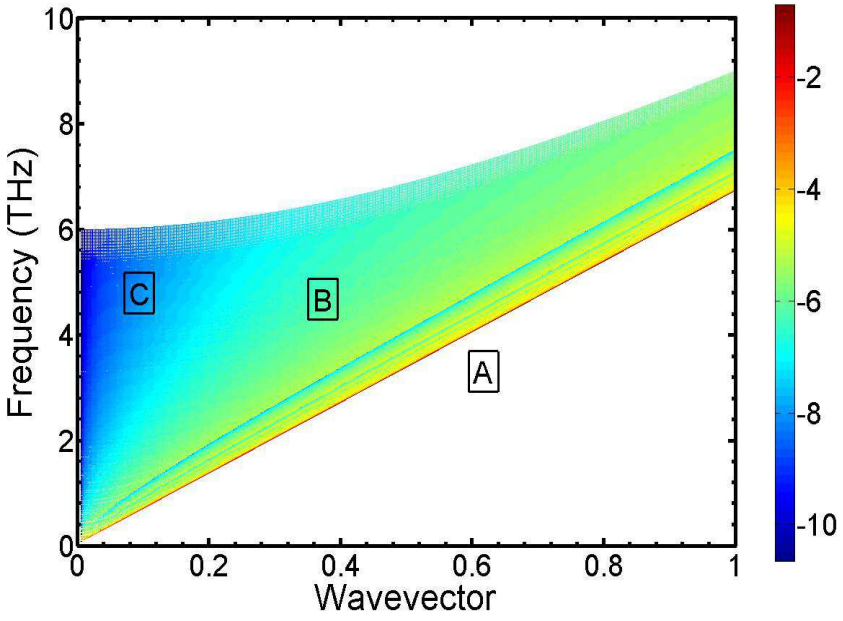

(a)

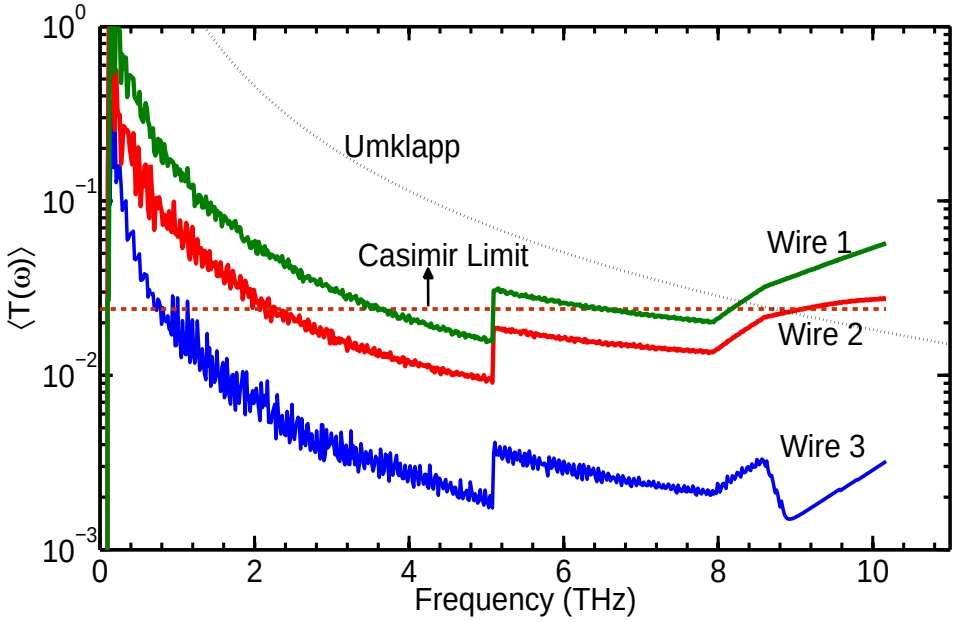

(b)

FIG. 1. (a) The logarithm of attenuation length plotted on phonon dispersion plot shows (A) quasi-ballistic transport for modes near fundamental branches (B) diffuse modes and (C) non-conducting modes near the zone center with high transverse wavenumbers. (b) The boundary scattering transmission coefficient for longitudinal modes averaged over number of modes is shown for wire 1 (σ=0.8 nm, L_c=300 nm), wire 2 (σ=2.5 nm, L_c=90 nm) and wire 3 (σ=2.5 nm, L_c=30 nm) for a 50 nm wire representing transition from smooth to very rough surface. The Casimir transmission ($=d/L$) and the Umklapp transmission($=\Lambda_u/L$) are also shown.

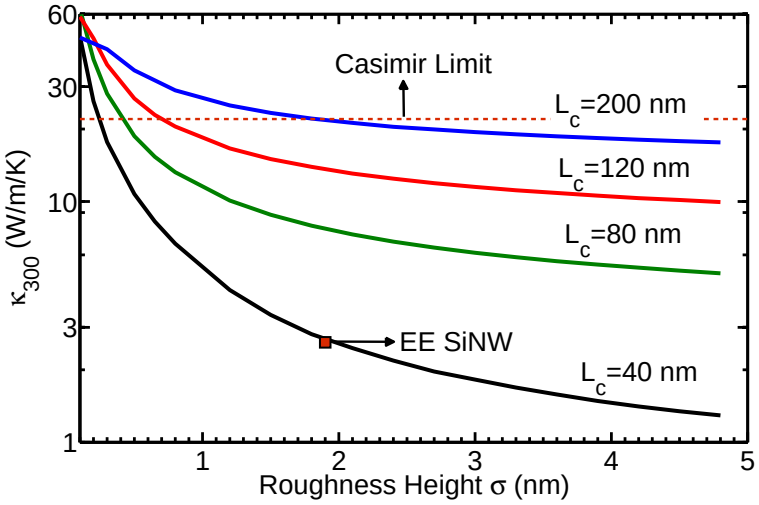

(a)

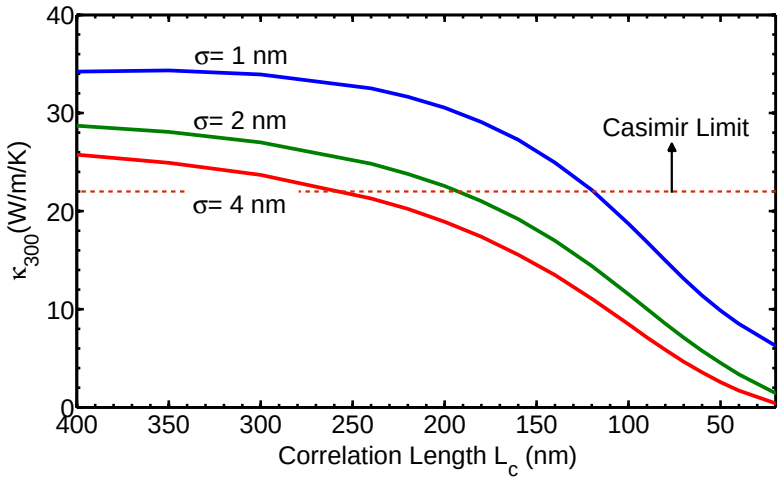

(b)

FIG. 2. Dependence of thermal conductivity at 300 K on (a) roughness height at different correlation lengths (b) correlation length at different roughness heights for a 50 nm wire, 2μm in length

.

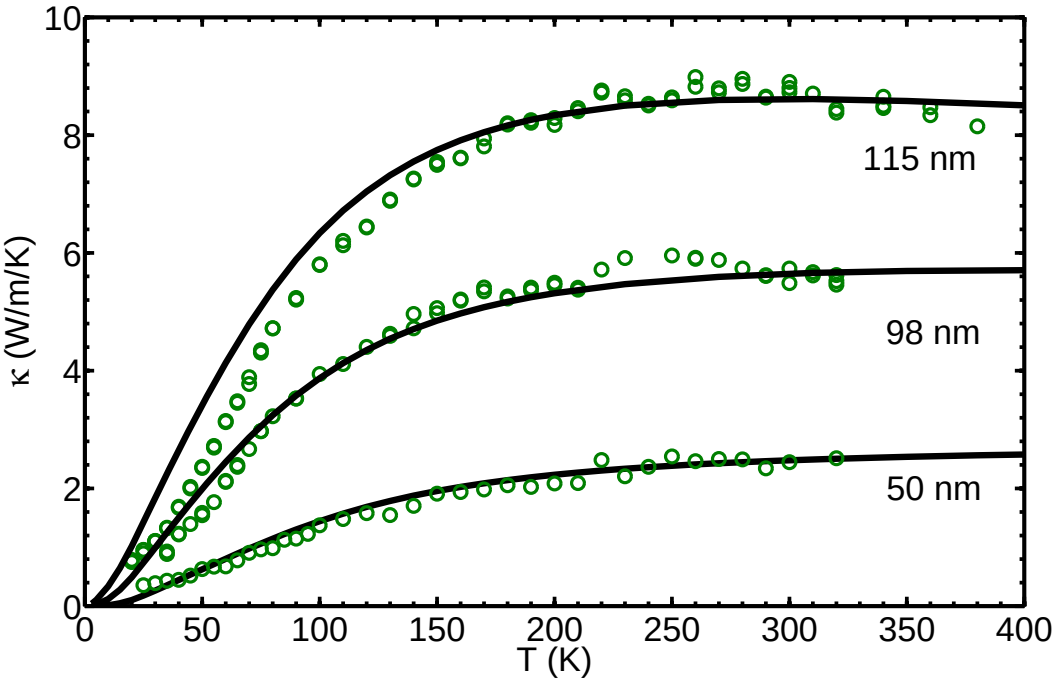

FIG. 3. Temperature trend of thermal conductivity of EE SiNW for 50 nm ($\sigma = 2.2$ nm, $L_c = 21$ nm), 98 nm ($\sigma = 2.2$ nm, $L_c = 70$ nm) and 115 nm ($\sigma = 2$ nm, $L_c = 86$ nm) diameter wires. The experimental data is from Ref[1].

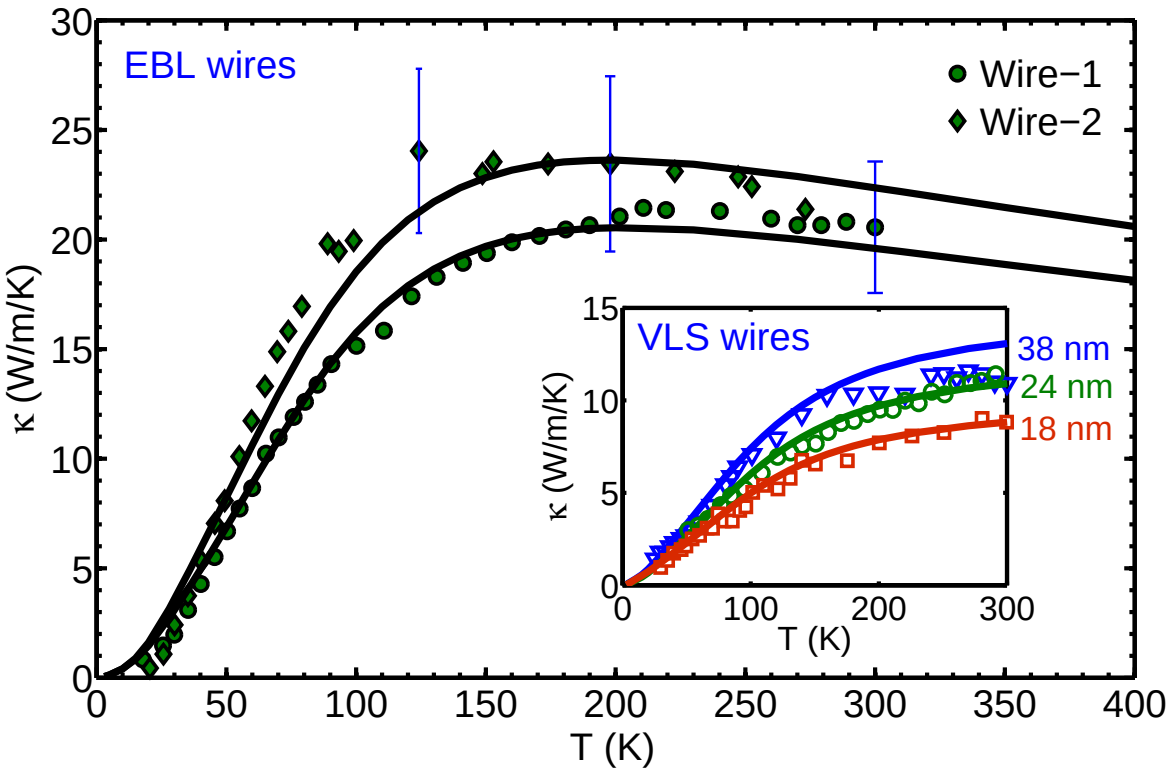

FIG. 4. Temperature trend of thermal conductivity of EBL wires using $\sigma = 7.4$ nm and $L_c = 400$ nm for Wire-1 ($120\times$ 41 nm^2 and $L = 4\mu m$) and Wire-2 (86×62 nm^2 and $L = 7\mu m$). The data is from Ref 2. (*Inset:* Temperature trend of thin VLS wires compared against data from Ref 7) using $\sigma = 1$ nm, $L_c = 80$ nm).